



Short communication

## New covalent salts of the 4+ V class for Li batteries

Leszek Niedzicki<sup>b</sup>, Sylvie Grugeon<sup>a</sup>, Stéphane Laruelle<sup>a</sup>, Patrick Judeinstein<sup>c</sup>, M. Bukowska<sup>a,b,c</sup>, J. Prejzner<sup>b</sup>, P. Szczeciński<sup>b</sup>, Władysław Wieczorek<sup>b</sup>, Michel Armand<sup>a,\*</sup>

<sup>a</sup> Université de Picardie Jules Verne, Laboratoire de Réactivité et de Chimie des Solides, 33 Rue Saint-Leu, F-80039 Amiens Cedex, France

<sup>b</sup> Warsaw University of Technology, Faculty of Chemistry, 00-664 Warszawa, ul. Noakowskiego 3, Poland

<sup>c</sup> Institut de Chimie Moléculaire et des Matériaux d'Orsay (UMR 8182), Bâtiment 410, Université Paris-Sud, F-91405 Orsay Cedex, France

### ARTICLE INFO

#### Article history:

Received 27 January 2011

Received in revised form 6 April 2011

Accepted 6 June 2011

Available online 24 June 2011

#### Keywords:

Lithium salt

Nonaqueous electrolyte

Li-ion battery

Hückel anion

### ABSTRACT

There is urgent action required for replacing LiPF<sub>6</sub> as a solute for Li-ion batteries electrolytes. This salt, prone to highly Lewis acidic PF<sub>5</sub> release and hydrolysis to HF is responsible for deleterious reaction on carbonate solvents, corrosion of electrode materials leading to safety problems then release to toxic chemicals. A major advantage of LiPF<sub>6</sub> is that it passivates aluminium. Most attempts to replace LiPF<sub>6</sub> with hydrolytically-stable salts have been unsuccessful because of Al corrosion.

We present here two “Hückel” type salts, namely lithium (2-fluoroalkyl-4,5-dicyano-imidazolate); fluoroalkyle = CF<sub>3</sub> (TDI), C<sub>2</sub>F<sub>5</sub> (PDI) with high charge delocalization. These thermally stable salts give both appreciably conductive solutions in EC/DMC (>6 mS cm<sup>-1</sup> at 20 °C) with a lower decrease with temperature than LiPF<sub>6</sub>. Non fluorinated lithium (4,5-dicyano-1,2,3-triazolate) is comparatively less than half as conductive. The lithium transference number *T*<sub>+</sub> measured by PFG-NMR is also higher. Voltammetry scans with either platinum or aluminium electrodes show an oxidation wall at 4.6 V versus Li<sup>+</sup>:Li<sup>0</sup>. These two salts are thus the first examples of strictly covalent, non-corroding salts allowing 4+ V electrode material operation. This is demonstrated with experimental Li/LiMn<sub>2</sub>O<sub>4</sub> cells as beyond the third cycles, the fade of the three electrolytes were quasi-identical, though LiPF<sub>6</sub> had a sharper initial decrease.

© 2011 Elsevier B.V. All rights reserved.

### 1. Introduction

The electrolyte is arguably the most critical component in batteries, as it should maintain its functions in contact with both the reducing negative electrode and oxidizing positive. This is especially true for lithium batteries where a 4+ V voltage span inevitably depends on the metastability of the electrolyte versus at least one electrode. Great hopes now rest on these batteries, beyond their undeniable success in portable electronic, with scale-up to a progressive electrification of transportation modes to EVs, HEVs and plug-in HEVs. Most of the research effort came after the first practical “Lithium-ion” (LIB) technology in 1991, where Li<sup>+</sup> is shuttled between two intercalation compounds, now established mainly as graphite (–) and cobalt-based layered oxides (+), manifestly the most extreme voltages that can be operated “safely”, though the list of incidents due to runaway reactions becomes longer with @ 10<sup>9</sup> batteries in operation. The miracle(s) taking place within batteries 10–100 g is unlikely to scale-up for the 200 Kg of an EV. Mixture of carbonates, and LiPF<sub>6</sub> as solute are used in the quasi-totality of LIBs because of their high conductivity, but the determining factor

is the absence of corrosion of aluminium current collectors at high anodic voltages (>4.5 V vs. Li<sup>+</sup>:Li<sup>0</sup>), i.e. well beyond the thermodynamic potential (1.3 V), and no other metal can offer a substitute in terms of cost, weight and malleability. The drawbacks of LiPF<sub>6</sub> are severe: (i) the high conductivity is relative as the transport number is low [1]; (ii) the tendency to dissociate into LiF and PF<sub>5</sub> with the latter inducing cationic chemistry deleterious to electrolyte; (iii) the facile hydrolysis to HF, inducing corrosion of the cathode materials, for instance Mn dissolution in LiMn<sub>2</sub>O<sub>4</sub>. The leached-out species after diffusing to negative electrode modify the SEI, raising its impedance, with resulting overheating and dramatic safety issues; (iv) combustion releases copious amount of HF; (v) less spectacular than a fire, smouldering, i.e. the reaction at high temperature with ethylene carbonate yields a derivative of fluoroethanol, a family of exceedingly toxic (LD 50 = 0.5 mg kg<sup>-1</sup> in mice) chemicals [2].

Of the possible substitutes for LiPF<sub>6</sub>, none of the classical LiAsF<sub>6</sub>, LiSbF<sub>6</sub>, LiClO<sub>4</sub> are close to meeting safety or innocuousness requirement. The “designer” anion [(CF<sub>3</sub>SO<sub>2</sub>)<sub>2</sub>N]<sup>-</sup> developed for polymer electrolytes (now also successful as ionic liquid component) would be ideal, except its crippling lack of aluminium protection. Conversely, the coordination anion, (bisoxalato)boron (BOB) ion, does passivate aluminium, but oxidises with gas evolution (CO<sub>2</sub>) specially above room temperature. Besides, the high rigidity/bulk of the molecule induces unfavourable phase diagrams at low

\* Corresponding author. Tel.: +33 322827881; fax: +33 322827590.

E-mail addresses: [stephane.laruelle@u-picardie.fr](mailto:stephane.laruelle@u-picardie.fr) (S. Laruelle), [michel.armand@u-picardie.fr](mailto:michel.armand@u-picardie.fr) (M. Armand).

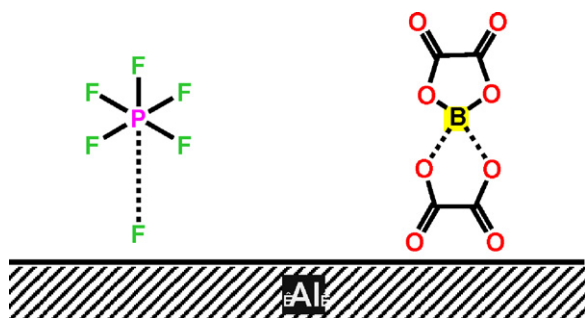


Fig. 1. Scheme of Al passivation with labile coordination salts.

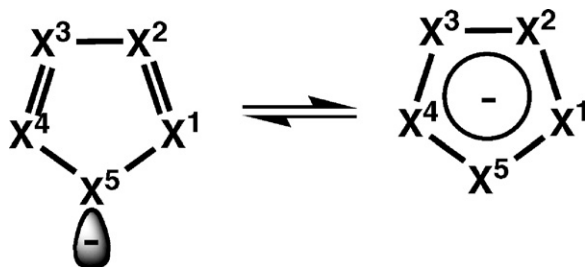


Fig. 2. The structure of "Hückel" anions: X = N, CCN, CCR<sub>F</sub>, etc.

temperature. Conventional wisdom suggests that the lability of F<sup>-</sup> and C<sub>2</sub>O<sub>4</sub><sup>2-</sup> from PF<sub>6</sub><sup>-</sup> resp. BOB<sup>-</sup> is the reason for passive film formation (Fig. 1). A promising substitute for LiPF<sub>6</sub> is Li[FSO<sub>2</sub>NSO<sub>2</sub>F] (LiFSI) which does not corrode aluminium up to at least 4 V. The cleavage of the S–F bond, (though more covalent than P–F) suggests that the passivating layer on Al is AlF<sub>3</sub>, a compound with high lattice energy, and used in microelectronics to protect Si for F-plasma etching. In similarity, the oxalate anion whose chelate "pincer" gap is more adapted to Al than B radii, would adsorb also (Fig. 1).

The question thus is the existence of a truly covalent anion, not prone to hydrolysis and irreversible HF, yet able to form a passivating layer on Al<sup>0</sup>, or at least preserve the native Al<sub>2</sub>O<sub>3</sub> layer. Several years ago, we have introduced the concept of "Hückel anions" [3] (Fig. 2), i.e. the delocalization of 6 "π" electrons on an aromatic 5-membered ring. A wealth of compounds with ring nitrogen and/or CN in the periphery [4,5] have been modelled and show very weak Li<sup>+</sup>–anion interactions, especially as the CN substitution increases. The simple representative, 4,5-dicyano-1,2,3-triazole (DCTA) has favourable conductivities in PEO electrolytes [6]. To further increase the resistance to oxidation and lessen the ion-pair formation, replacement of central N by C–CF<sub>3</sub> or C<sub>2</sub>F<sub>5</sub> to 4,5-dicyano-2-trifluoromethyl-imidazole and 4,5-dicyano-2-pentafluoroethyl-imidazole (TDI and PDI respectively) has, also in PEO electrolytes, showed excellent conductivities and favourable phase diagram. No oxidation was seen before the polyether own limit (4 V) [6]. We inferred that these salts deserved further investigation in classical liquid electrolytes, as a covalent salt is of considerable technological advantage, without the release of a strong Lewis acid like PF<sub>5</sub> able to induce a series of deleterious reactions with solvent and avoid the formation of fluoroethanol derivatives, unacceptable for general application of EVs. These salts will be compared with the non-fluorinated LiDCTA and LiPF<sub>6</sub>.

## 2. Experimental

TDI and PDI are made in a one-pot reaction from commercial chemicals (Fig. 3) in respectively 55 and 50% yield [7,8]. The two white powders were dried at 150 °C for 12 h in a Büchi TO-50 oven

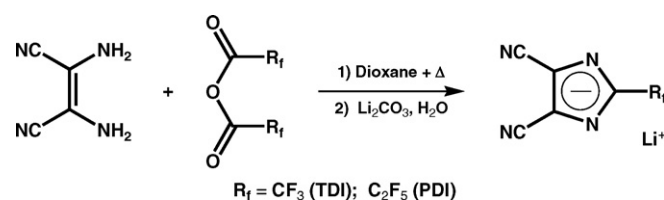


Fig. 3. Synthesis scheme for LiTDI and LiPDI.

prior to being used and kept in a dry box. LiDCTA was made from the reaction of diamino-maleonitrile with *tert*-butyl nitrite in diethyl ether at 0 °C for 48 h. The turbid yellow suspension was centrifuged and stripped from solvent. Crude 4,5 dicyanotriazole was sublimed in vacuum (80 °C) to obtain the pure acid. The Li salt was made in ethanol by reaction on 10% excess of Li<sub>2</sub>CO<sub>3</sub>, filtration and drying. LiPF<sub>6</sub> 1 M in EC/DMC (50/50, w/w) was obtained from Merck (LP30®).

Coupled thermogravimetric and DSC traces between RT and 300 °C under a constant flow of argon (50 ml min<sup>-1</sup>) were acquired with a Netzsch Jupiter STA 449C thermal analyser at a heating/cooling rate of 10 °C min<sup>-1</sup>. The isothermal drift and sensitivity values are 0.6 μg h<sup>-1</sup> and 0.1 μg, respectively. Aluminium crucibles were loaded with 25 mg of the salts and sealed in the dry box. A small hole was punched in the lid just prior to loading in the apparatus.

Conductivity measurements were performed using a CDC749 (Radiometer Analytical) cell. All the electrochemical experiments were conducted at 20 °C using a VMP3 system (Biologic S.A., Claix, France) with a 1 M lithium salt dissolved in EC/DMC (50/50, w/w) solvents mixture.

PGF-NMR diffusion measurements were carried out on 9.4 T Bruker Avance 400 NMR spectrometre equipped with a Bruker 5 mm broadband probe with a z-axis gradient and a temperature controller (stability and accuracy 0.2 °C). NMR resonance frequencies are 400.1 MHz, 376.50 MHz and 155.51 MHz respectively for <sup>1</sup>H, <sup>19</sup>F and <sup>7</sup>Li nuclei. The self-diffusion measurements were performed with the pulsed field gradient stimulated echo and LED sequence using 2 spoil gradients (PGF NMR) [9]. The magnitude of the pulsed field gradient was varied between 0 and 40 G cm<sup>-1</sup>, the diffusion time Δ between two pulses was fixed at 100 ms and the gradient pulse duration δ was set between 3 and 10 ms depending on the diffusion coefficient of mobile species. This allowed us to observe the attenuation of spin echo amplitude over a range of at least 2 decades leading to a good accuracy (<5%) of the self-diffusion coefficient values. They were determined from the classic relationship  $A/A_0 = \exp[-Dg^2\gamma^2\delta^2(\Delta - \delta/3)]$  where *g* is the magnitude of the two gradient pulses, γ is the gyromagnetic ratio of the nucleus under study and *A* and *A*<sub>0</sub> are respectively the area of the signal obtained with or without gradient pulses.

Cyclic voltammetry measurements were acquired at a scan rate of 30 mV s<sup>-1</sup>, in the 0.5–6 V or 0.01–6 V potential ranges (vs. Li<sup>+</sup>:Li<sup>0</sup>). An Al or Pt wire was used as working electrode, a Pt wire as counter electrode and metallic Li as reference electrode.

Galvanostatic tests were performed in Swagelok® cells using a plastic positive electrode on an Al disk containing 64 wt% LiMn<sub>2</sub>O<sub>4</sub>, 8 wt% SP carbon, and 28 wt% poly(vinylidene fluoride)-co-hexafluoropropylene (PVdF-HFP) copolymer binder (the electrode films were cast and processed using a procedure previously reported) [10], a 1 cm disk of Li foil as the negative electrode, and a Whatman GF/D borosilicate glass fibre mat separator. The electrode rate capability was determined via the collection of a signature curve as the function of the salt. After a low rate charging, the cell was successively discharged at decreasing rates (5 C, 2.5 C, 1 C, 0.5 C, C/5, C/10 and C/20) with a relaxation time of 30 min between each step.

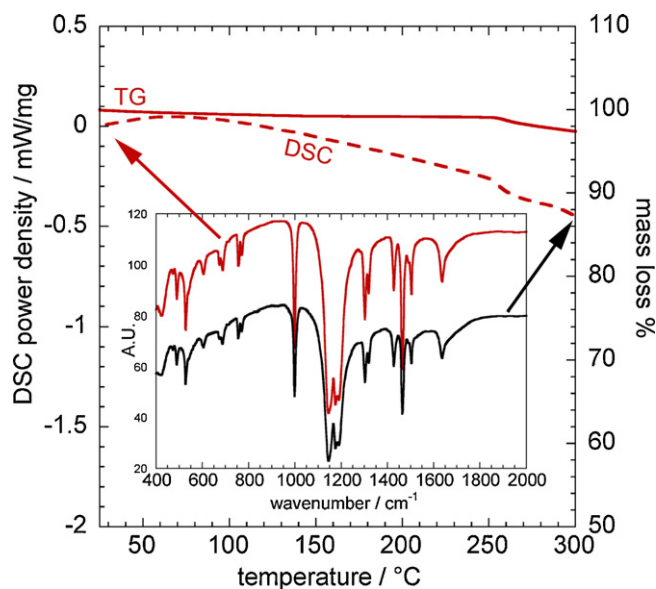


Fig. 4. TGA, DSC traces of LiTDI, heating scan at  $10^{\circ}\text{C min}^{-1}$  and IR spectra recorded before and after the scan.

### 3. Results and discussions

The two salts TDI and PDI are stable up to  $250^{\circ}\text{C}$  as shown by TGA-DSC. The TDI salt IR spectra recorded on the material dried at  $150^{\circ}\text{C}$  and  $300^{\circ}\text{C}$  are identical as shown in Fig. 4, showing that the material is chemically stable; PDI, (not shown) behaves similarly. 1 M solutions were prepared from EC/DMC (50/50, w/w) mixture inside the dry box. Karl-Fisher measurements performed on the solution showed a water content of 20 ppm, when the drying temperature was  $150^{\circ}\text{C}$  and this treatment was kept for all batches used in this study except  $\text{LiPF}_6$ .

The conductivity of such solutions was measured at  $20^{\circ}\text{C}$  and is summarized in Table 1: for comparison,  $\text{LiTFSI}$ , dicyanotriazole (DCTA) anions salts were measured. The TDI and PDI salts display quite similar conductivities in the  $[-20\text{ }^{\circ}\text{C}$  to  $+45^{\circ}\text{C}]$  temperature span (Fig. 5). All salts obey a free-volume law, and the decrease in conductivity when lowering the temperature is slightly lower for the Hückel salts. Crystallisation with time (precipitation of EC) does not take place with the latter salts at  $-20^{\circ}\text{C}$ , but is visible after a few hours for  $\text{LiBOB}$  a competitor salt, indicating a better phase diagram. These salts are much more conductive than DCTA, with only  $\text{LiPF}_6$  and  $\text{LiTFSI}$  showing higher performances, and comparable with  $\text{LiBOB}$  ( $7.5\text{ mS cm}^{-1}$  at  $0.7\text{ M}$ ).

Table 1  
Conductivity of various salts 1 M in EC/DMC (50/50, w/w)  $T=20^{\circ}\text{C}$ .

Solute	$\sigma$ ( $\text{mS cm}^{-1}$ )
$\text{LiPF}_6$	10.8
$\text{LiTFSI}$	9.0
$\text{LiTDI}$	6.7
$\text{LiPDI}$	6.3
$\text{LiDCTA}$	2.7

Table 2  
PFG-NMR diffusion coefficients for  $\text{Li}^+$ , anion, EC and DMC and transport numbers for  $\text{Li}^+$ ;  $T=25^{\circ}\text{C}$ .

	$D_{\text{cation}}$ ( $\text{cm}^2\text{ s}^{-1}$ )	$D_{\text{anion}}$ ( $\text{cm}^2\text{ s}^{-1}$ )	$D_{\text{solvent}}$ ( $\text{cm}^2\text{ s}^{-1}$ )	$T_+$
$\text{LiPF}_6$ (LP30 <sup>®</sup> )	$2.45 \times 10^{-6}$	$3.50 \times 10^{-6}$	$4.59 \times 10^{-6}$ (EC) $5.97 \times 10^{-6}$ (DMC)	0.41
$\text{LiTDI}$	$2.21 \times 10^{-6}$	$2.57 \times 10^{-6}$	$4.59 \times 10^{-6}$ (EC) $5.79 \times 10^{-6}$ (DMC)	0.46
$\text{LiPDI}$	$2.14 \times 10^{-6}$	$2.53 \times 10^{-6}$	$4.82 \times 10^{-6}$ (EC) $6.36 \times 10^{-6}$ (DMC)	0.46

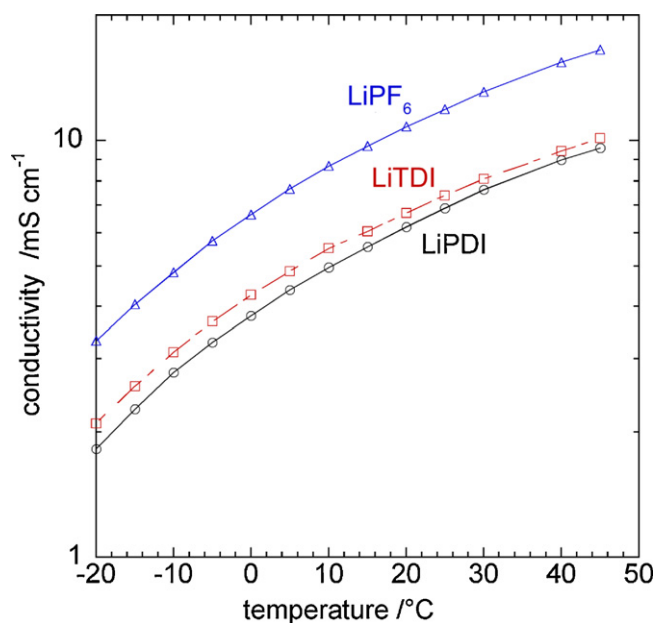
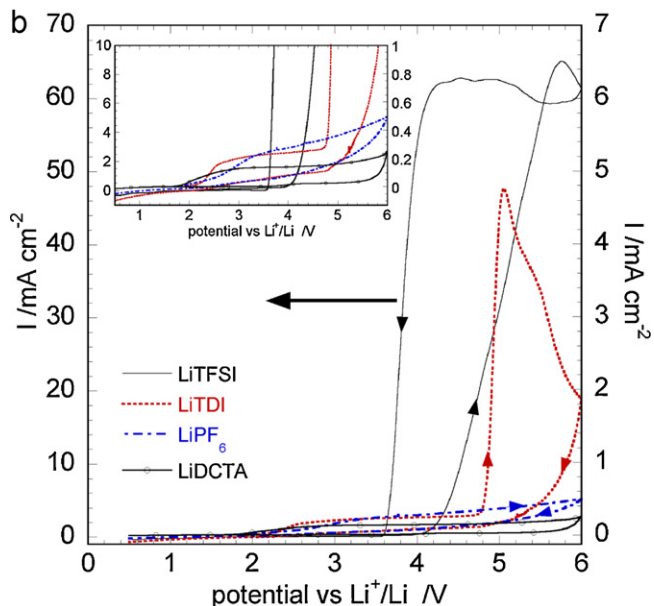
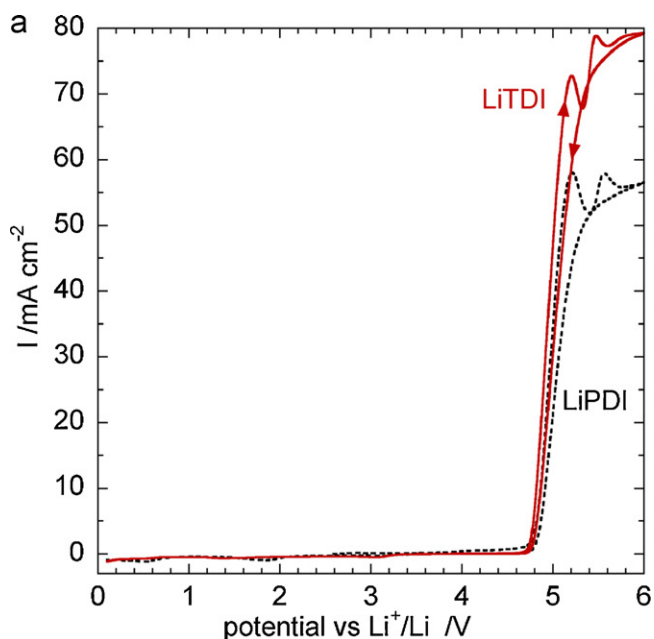


Fig. 5. Conductivity of 1 M  $\text{LiPF}_6$ ,  $\text{LiTDI}$  and  $\text{LiPDI}$  salts in EC/DMC (50/50, w/w) as a function of the temperature.

The Vincent & Bruce polarization for  $T_+$  estimation [11] relies on the hypothesis that this value is independent of concentration and assimilates activities with concentrations. The NMR measurement of transport numbers is immune to such criticism, as no chemical gradient is created. The diffusion coefficients obtained by PFG-NMR for the different transport numbers are summarized in Table 2 and the cationic transport numbers are calculated by definition as  $T_+ = D_{\text{cation}} / (D_{\text{cation}} + D_{\text{anion}})$  assuming the validity of the Nernst-Einstein equation. Table 2 contains also the diffusion coefficients for the two components of the solvent ( $^1\text{H}$  NMR resonances of linear DMC and cyclic EC are respectively at 3.3 and 4.2 ppm).

As can be seen from this data, the transport number of lithium cations with both TDI and PDI anions are higher than that for  $\text{PF}_6^-$ . The larger diffusion coefficient for the less polar DMC solvent is a favourable feature, this faster moving molecule leaving behind high- $\epsilon$  EC, a better solvent for concentrated salt solutions at the negative (on discharge) and positive (on charge). It is interesting to note that the  $T_+$  value is the same for both TDI and PDI, despite the larger volume of the latter. This, once again, shows that the relative mobilities of anions are determined by their chemical structure and charge delocalization as was showed earlier in the  $\text{Li}[\text{R}_f\text{SO}_3]$  and  $\text{Li}[(\text{R}_f\text{SO}_2)_2\text{N}]$  ( $\text{R}_f = \text{C}_n\text{F}_{2n+1}$ ,  $1 \leq n \leq 4$ ) systems [12,13] independently on their size. The role of the anion in the close environment of the cation is also reflected by the different chemical shifts of  $\text{Li}^+$ ,  $\delta = -0.81$ ,  $-0.46$  and  $-0.58$  ppm for  $\text{PF}_6^-$ , TDI and PDI respectively.

The voltage stability window of the electrolyte had been tested on Pt electrode as shown in Fig. 6a. The supporting solvents are stable or metastable to @ 6V over the short time of the cyclic voltammetry and the PDI and TDI anions show good stability until 4.80 V versus  $\text{Li}^+:\text{Li}^{\ominus}$  followed by an oxidation wall which is similar for both anions, reflecting the similar electronic structure of the charge-bearing ring.



**Fig. 6.** (a) Cyclic voltammogram of 1 M LiTDI and LiPDI in EC/DMC (50/50, w/w), on Pt electrode at  $30 \text{ mV s}^{-1}$ , upper cut-off 6 V (vs.  $\text{Li}^+:\text{Li}^0$ ). (b) Cyclic voltammogram of LiTDI,  $\text{LiPF}_6$ ,  $\text{Li}[\text{CF}_3\text{SO}_2]_2\text{N}$  and LiDCTA, all 1 M in EC/DMC (50/50, w/w), on Al electrode. Voltage limits are 0.1–6 V (vs.  $\text{Li}^+:\text{Li}^0$ ), scan speed  $30 \text{ mV s}^{-1}$ .

When Pt is replaced by an aluminium wire (Fig. 6b), TDI (and PDI not shown for clarity) oxidize at about the same potential of 4.75 V, and the current before this threshold and the return current are negligible, almost similar to that found for  $\text{LiPF}_6$  in commercial LP30<sup>®</sup>. For comparison, LiTFSI undergoes a large corrosion current beyond 3.3 V, practically an order of magnitude larger than the oxidation wall of TDI. LiDCTA was also tested, and shows also very little corrosion up to 6 V. Thus the three Hückel rings, ( $\neq \text{LiPF}_6$ ), either passivate the Al surface, or keep intact the native  $\text{Al}_2\text{O}_3$  layer on this metal and are the first totally covalent anions showing this necessary property. The absence of dissolution of native  $\text{Al}_2\text{O}_3$  probably applies to PDI and TDI, while DCTA anion, devoid of electron-withdrawing fluorine, is calculated to oxidize  $\approx 4 \text{ V}$  versus  $\text{Li}^+:\text{Li}^0$  and thus the low current is attributed to an insoluble protecting layer.

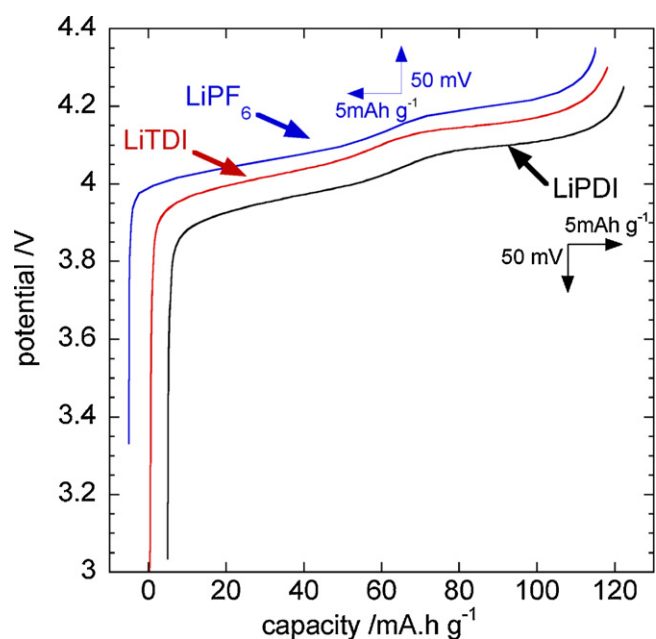


**Fig. 7.** Charge behaviour for  $\text{LiMn}_2\text{O}_4$  with LiTDI, LiPDI and  $\text{LiPF}_6$ , all 1 M in EC/DMC (50/50, w/w); upper cut-off 4.3 V. For legibility, LiPDI and  $\text{LiPF}_6$  traces are shifted by  $5 \text{ mAh g}^{-1}$  and 50 mV.

When a Swagelok<sup>®</sup> cell laden with 7 mg of  $\text{LiMn}_2\text{O}_4$ , and carbon is charged (C/20) to 4.3 V (Fig. 7) the theoretical capacity for this voltage upper limit is obtained ( $\approx 120 \text{ mAh g}^{-1}$ ) with both salts, without any visible side reactions for the electrochemical delithiation. The knee at 4.1 V is typical of  $\text{Li}^+$  ordering in the spinel structure ( $x \approx 0.5$  in  $\text{Li}_x\text{Mn}_2\text{O}_4$ ).

The cycling behaviour at C/10 was compared between LiTDI, LiPDI and LP30 electrolytes in the same Swagelok cells. As evident from Fig. 8, the cells behave quite promisingly, with a fade on the first 25 cycles at an average of 3% per cycle, as compared with 5% for  $\text{LiPF}_6$  in the same conditions, though the initial capacity with  $\text{LiPF}_6$  was slightly higher. It should be stressed that the upper limit (4.3 V) for these cycling tests is above that of commercial cells using the manganese spinel phase. However, the TDI and PDI ( $\approx 95\%$ ) coulombic efficiencies are lower than for  $\text{PF}_6$  ( $\approx 98\%$ ). We believe that the relatively inefficient C/D may be due to losses to build the passivation layer on Al and  $\text{LiMn}_2\text{O}_4$ .

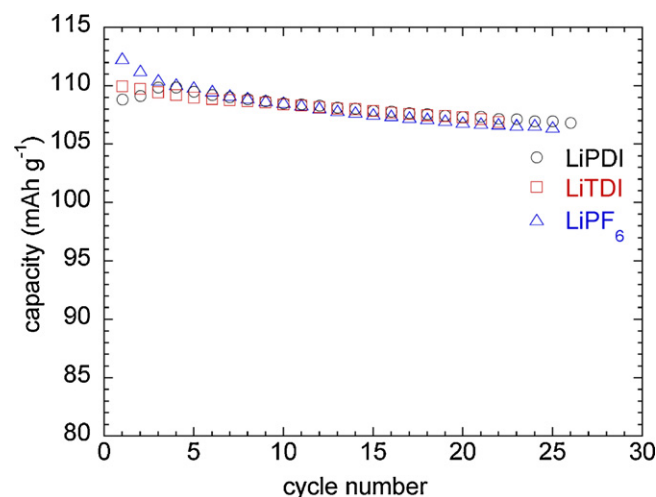


**Fig. 8.** Discharge capacity retention of  $\text{LiMn}_2\text{O}_4$  electrode with 1 M LiTDI, LiPDI and  $\text{LiPF}_6$  in EC/DMC (50/50, w/w); upper/lower cut-off 4.3/3.5 V (vs.  $\text{Li}^+:\text{Li}^0$ ).

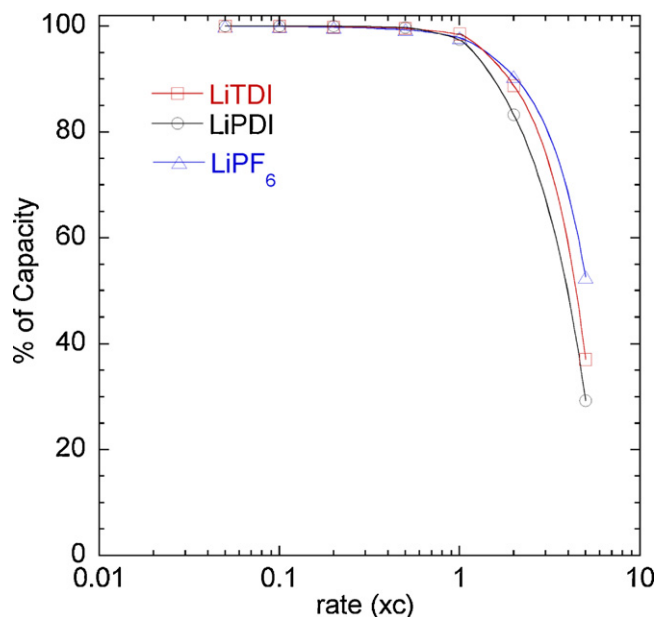


Fig. 9. Signature curve of  $\text{LiMn}_2\text{O}_4$  electrode with 1 M LiTDI, LiPDI and  $\text{LiPF}_6$  in EC/DMC (50/50, w/w).

Finally, the power capability of these new salts was evaluated in the same type of cell configuration. The interpretation of such experiments should always be done with caution when comparing different cathode materials. Here, with a “fast” electrode (typical grain size  $\approx 0.5 \mu\text{m}$ ) material like  $\text{LiMn}_2\text{O}_4$ , there is no ambiguity that the signature curve in Fig. 9 reflects the lithium throwing power of the electrolytes, again dependent of the total conductivity and of the transport number. The two salts compare quite well with  $\text{LiPF}_6$ , especially TDI with all the capacity available at 1 C rate. For application, we also tested the wettability of LP30 and LiTDI/EC/DMC electrolytes with polyethylene separator and found that the contact surface was larger in case of LiTDI base electrolyte; the low surface energy being certainly brought by the  $\text{CF}_3$  group.

#### 4. Conclusion

The two new salts based on the negatively charged imidazole ring rendered more dissociated by two “ $\pi$ ” strongly electron-withdrawing cyano groups and one “ $\sigma$ ” EWG  $\text{CF}_3$  – or  $\text{C}_2\text{F}_5$  – or namely TDI and PDI have been tested as substitutes for  $\text{LiPF}_6$  in conventional carbonate solvents. The comparisons are quite positive, as these salts, totally covalent and not prone to hydrolysis, protect

aluminium from corrosion up to potential that are not reached in conventional batteries. This is against conventional wisdom that links the formation of protective  $\text{AlF}_3$  to facile release of  $\text{F}^-$  by the anion, which is not the case. There is no explanation yet for the formation of a protective film (or the preservation of the native  $\text{Al}_2\text{O}_3$  film) in the presence of TDI or PDI. DCTA, the non-fluorinated analogue, also passivates aluminium, but its conductivity is only 40% of that of TDI.

On all tests, the two salts give good performances, and the only drawback is a slightly smaller conductivity and its consequence on the power capability. It must be stressed however that the optimum in lithium transport (EC/DMC ratio, concentration, etc.) have not been sought for. Also, after several cycles, the growth of the SEI and its possible contamination by Mn ( $\text{LiMn}_2\text{O}_4$ ) or Fe (low quality  $\text{FePO}_4$ ) dissolved in the presence of  $\text{LiPF}_6$  is the major source of impedance, not the electrolyte conductivity. In the last instance, the incineration of the battery in case of accidental fire would, with TDI, release only half of the HF compared to  $\text{LiPF}_6$  and batteries with these Hückel salts are expected to be safer, as immune from the dissociation equilibria occurring in the latter with the release of  $\text{PF}_5$  and HF from its hydrolysis.

#### Acknowledgements

The authors thank Matthieu Courty for the DSC/TGA experiment and Dr. Murata (Nippon Shokubai, Japan) for providing a sample of LiDCTA to which our synthesis was compared.

#### References

- [1] S. Stewart, J. Newman, *J. Electrochem. Soc.* 155 (2008) A458.
- [2] A. Hammami, N. Raymond, M. Armand, *Nature* 424 (2003) 635–636.
- [3] C. Michot, M. Armand, M. Gauthier, Y. Choquette, Patent WO/1998/029399 (1998).
- [4] P. Johansson, H. Nilsson, P. Jacobson, M. Armand, *Phys. Chem. Chem. Phys.* 6 (2004) 5.
- [5] P. Johansson, S. Béranger, M. Armand, H. Nilsson, P. Jacobsson, *Solid State Ionics* 156 (1–2) (2003) 129–139.
- [6] M. Egashira, B. Scrosati, M. Armand, S. Béranger, C. Michot, *Electrochem. Solid State Lett.* 6 (4) (2003) A71–A73.
- [7] L. Niedzicki, G.Z. Żukowska, M. Bukowska, P. Szczeciński, S. Gurgeon, S. Laruelle, M. Armand, S. Panero, B. Scrosati, M. Marcinek, W. Wieczorek, *Electrochim. Acta* 55 (2010) 1450–1454.
- [8] L. Niedzicki, M. Kasprzyk, K. Kuziak, G.Z. Żukowska, M. Armand, M. Bukowska, M. Marcinek, P. Szczeciński, W. Wieczorek, *J. Power Sources* 192 (2009) 612–617.
- [9] S. Altieri, D.P. Hinton, R.A. Byrd, *J. Am. Chem. Soc.* 117 (1995) 7566–7567.
- [10] J.-M. Tarascon, A.S. Gozdz, C. Schmutz, F. Shokoohi, P.C. Warren, *Solid State Ionics* 86 (1996) 49.
- [11] J. Evans, C.A. Vincent, P.G. Bruce, *Polymer* 28–13 (1987) 2324–2322.
- [12] W. Gorecki, P. Donoso, C. Berthier, M. Mali, J. Roos, D. Brinkmann, M. Armand, *Solid-State Ionics* 28–30 (1988) 1018.
- [13] W. Gorecki, C. Roux, M. Clémancey, M. Armand, E. Belorizky, *Chem. Phys. Chem.* 3 (7) (2002) 620–625.